Princeton Plasma Physics Laboratory

PPPL- 4530

PPPL- 4530

Measuring the Density of a Molecular Cluster Injector via Visible Emission from an Electron Beam

D.P. Lundberg, R. Kaita, R. Majeski, and D.P. Stotler

June, 2010

Prepared for the U.S. Department of Energy under Contract DE-AC02-09CH11466.

Princeton Plasma Physics Laboratory
Report Disclaimers

Full Legal Disclaimer

Trademark Disclaimer

PPPL Report Availability

Princeton Plasma Physics Laboratory:

http://www.pppl.gov/techreports.cfm

Office of Scientific and Technical Information (OSTI):

http://www.osti.gov/bridge

Related Links:

U.S. Department of Energy

Office of Scientific and Technical Information

Fusion Links

Measuring the Density of a Molecular Cluster Injector via Visible Emission from an Electron Beam[a)]

D.P. Lundberg,[b)] R. Kaita, R. Majeski, and D.P. Stotler

Princeton Plasma Physics Laboratory, P.O. Box 451, Princeton, New Jersey 08543

A method to measure the density distribution of a dense hydrogen gas jet is presented. A Mach 5.5 nozzle is cooled to 80K to form a flow capable of molecular cluster formation. A 250V, 10mA electron beam collides with the jet and produces H_α emission that is viewed by a fast camera. The high density of the jet, several $10^{16}\mathrm{cm}^{-3}$, results in substantial electron depletion, which attenuates the H_α emission. The attenuated emission measurement, combined with a simplified electron-molecule collision model, allows us to determine the molecular density profile via a simple iterative calculation.

[a)]Contributed paper, published as part of the Proceedings of the 18th Topical Conference on High-Temperature Plasma Diagnostics, Wildwood, New Jersey, USA, May 2010.

[b)]Electronic mail: dlundberg@pppl.gov

I. INTRODUCTION

Control of the fueling of fusion plasma experiments continues to be a challenge. Traditional methods, such as gas puffers at the plasma edge, produce relatively diffuse and low density gas clouds that do not penetrate far into the plasma.[1] Because the plasma density profile is sensitive to the fuel deposition profile,[2] it is necessary to develop high-density, well-collimated fueling sources that will deposit particles past the plasma separatrix. One possibility is a Molecular Cluster Injector (MCI), which is being developed to fuel the Lithium Tokamak eXperiment.[3] The MCI pre-cools the reservoir gas with liquid nitrogen and passes it through a supersonic nozzle. With an 80K reservoir temperature and a sufficiently high backing pressure, the jet that is produced satisfies the conditions for molecular cluster formation.[4] Clusters free stream in ballistic trajectories near the jet axis, yielding densities that persist over long distances from the nozzle.[5] There is evidence to suggest that this allows a larger fraction of the molecules to penetrate past the plasma edge.[6] However, to understand the interaction of the MCI with a plasma, it is necessary to characterize the density distribution of the supersonic flow it produces.

To achieve this, a new method of determining the density of a hydrogen jet was developed. The visible H_α emission produced by a 250V incident electron beam ("e-beam") is measured. The gas density is sufficient to cause significant depletion of the e-beam as it traverses the jet, due to electron-molecule collisions. Prior studies of e-beam fluorescence restricted e-beam depletion to less than 10%, to preserve a uniform electron density and energy. This limits the gas density to well under $\sim 10^{16}\text{cm}^{-3}$.[7] This work uses the attenuation of the visible emission due to e-beam depletion as high as 75% as a means to infer the absolute gas density. A simplified model for the interaction of the electrons and hydrogen molecules is used, but this method could in principle be extended to other gases. The electron-induced emission gives a non-invasive measurement of the density distribution, with spatial resolution of 0.1cm and sub-millisecond temporal resolution. This article presents example MCI density profiles recovered from the H_α emission of a substantially depleted e-beam.

II. METHOD

A 250V, 10mA e-beam intersects the hydrogen gas jet produced by a Parker Series 99 fast solenoid valve (see Figure 1). The valve orifice is 0.01" in diameter, and is fitted with a 4.5° conical nozzle that opens to a 0.125" outlet diameter, yielding a design Mach number of 5.5. The valve is mounted on a bellows to allow motion in the z-direction, and is surrounded by a copper jacket which is cooled with liquid nitrogen to 80K. The electron source consists of a tungsten filament, heated with a Thermionics e-Gun supply, and biased negative relative to a collimating anode via an HP-711 supply. The experiments take place in a 177 liter vacuum tank, pumped to 10^{-6} torr. The pressure rise in the tank is held below a few tens of millitorr by limiting the valve opening time to 4-8ms, so that the e-beam is unperturbed when it arrives at the gas jet. The e-beam travels in the x-direction in Figure 1, and is confined by a 75 gauss guide field. The electrons collide with hydrogen molecules and excite emission that is viewed with a Vision Research Miro II fast camera, through an H_α filter with a 1.5nm bandpass.

The valve is backed with 50-150psia of hydrogen, which, combined with the 80K reservoir temperature and the high Mach number nozzle, is sufficient to produce significant numbers of clusters.[4] Clusters with 10^3 molecules or more have reduced optical emission relative to an equal number of gas molecules, due to a smaller effective excitation cross-section and local quenching of excited atoms.[8] Furthermore, the effective electron-impact ionization cross-section is reduced for large clusters,[9] which may affect the depletion rate of the electron beam. However, the clusters formed in the supersonic jets measured in this work are expected to consist of 100 or fewer molecules each,[10] so their emission characteristics are indistinguishable from individual molecules. If the valve were backed with pressures in excess of 300psia, or if a liquid helium cooling system were employed, the resulting flows could contain clusters of at least 10^3 molecules, and the measurement technique outlined below would need to account for a reduced electron-impact ionization cross-section and atomic emission efficiency.

We now discuss the relevant electron-molecule collision processes that result in emission and beam depletion, present a simplified model for the system, and demonstrate how to determine the H_2 density from the H_α emission. The e-beam free streams until it encounters the gas jet and collides with H_2 molecules. Collision products, such as atoms, molecular ions, and excited molecules leave the interaction region faster than subsequent collisions

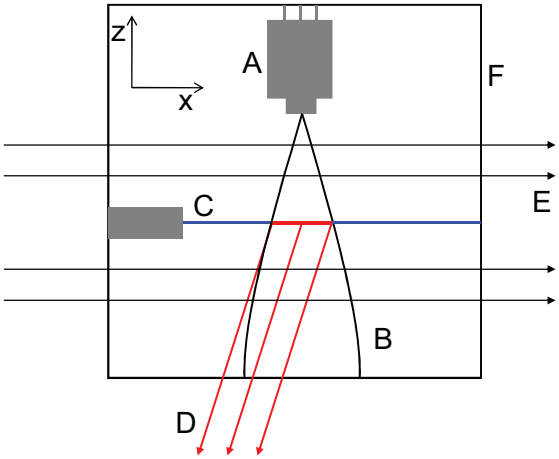

FIG. 1. (Color online) The solenoid valve and nozzle (A), produce a collimated gas jet (B). The electron beam (C) collides with the jet, producing emission (D) that is viewed by a fast camera. The beam is confined by a 75 gauss magnetic field (E), and the experiment is contained in a 177 liter vacuum tank (F)

can occur. As a result, multi-step excitation and ionization processes are rare, and the H_α emission is primarily produced by electron collisions with ground state molecules. The molecular density is high, $\sim 10^{16}\text{cm}^{-3}$, and the e-beam density is low, $5 \times 10^{9}\text{cm}^{-3}$, so that even in cases where every electron undergoes multiple collisions, this is a non-invasive measurement of the H_2 density. The three major reactions in the system are: 1) ionization, accounting for 80% of the total for electron energies over $\sim$ 30eV, 2) dissociative ionization, a 5% contribution, and 3) dissociation, comprising 15% of the total, except at electron energies below 10eV, where it is dominant.[11] While the degree of beam depletion is due to the sum total of these processes, the H_α emission results solely from $H^*(n=3)$ atoms produced by dissociative excitation:

$$e^- + H_2 \rightarrow e^- + H(n=1) + H^*(n=3) \tag{1}$$

with the collision cross section σ_{de3}. The Einstein coefficient for H_α is $A_{32} = 4.41 \times 10^7 s^{-1}$, during which the 2-3eV $H^*(n=3)$ product atoms travel less than 0.03cm. Because the camera resolution is 0.1cm, the intensity of H_α viewed by the camera, $I(x,z)$, is a valid local measurement of the $H^*(n=3)$ source rate. $I(x,z)$ is then proportional to the product of

the local electron and molecular densities:

$$I \propto \left(\frac{dn_{H^*(n=3)}}{dt}\right)_{source} = n_e n_{H2} \sigma_{de3} v_e \tag{2}$$

where v_e is the electron velocity. In general, if n_e, σ_{de3}, and v_e are known, this allows an absolute determination of n_{H2}. For example, if the vacuum tank is pre-filled with a known n_{H2}, and I is measured, this yields a calibration of camera counts per number density of hydrogen. If the same camera and e-beam parameters are used, the absolute n_{H2} profile of the gas jet can then be inferred from $I(x, z)$, but only if the e-beam energy and density are not significantly modified across the width of the jet. This approach fails when the gas density reduces the mean free path of an electron to the scale of the gas jets of interest, which is generally $\sim$ 5cm. For e-beams of a few hundred volts, this density threshold is $\sim 2 \times 10^{15}\text{cm}^{-3}$. To study jets of higher density, it is necessary to consider electrons that undergo multiple collisions. The e-beam density, energy, and emission cross section are no longer necessarily constant. Figure 2a contains $\sigma_{de3} v_e$ for the energy range 18-250eV.[11] $\sigma_{de3} v_e$ has a weak variation from 50-250eV, and falls off sharply below 50eV. To simplify the description of the emission process, $\sigma_{de3} v_e$ can be approximated by a step function, so that electrons cause emission with the average value of $8.27 \times 10^{-10}\text{cm}^{-3}\text{s}^{-1}$ for 34-250eV, and do not cause emission below 34eV.

We now consider the process of beam depletion. For electrons moving a differential distance between points x_i and x_{i+1} through a background neutral density n_n, the single-collision penetration of electrons is described by the flux, $\Gamma(x_{i+1}) = n_e(x_{i+1})\, v_e(x_{i+1}) = n_e(x_i)\, v_e(x_i)\, e^{-(x_{i+1}-x_i) n_n(x_i) \sigma}$, where σ is the collision cross-section.[12] The diagnostic described in this work only measures the subset of electrons that can cause H_α emission. With the step-function approximation in Figure 2a, the emission process for electron energies above the emission threshold of 34eV is independent of energy, and by extension, velocity. If the collision processes that deplete the emitting population are also approximated as independent of the electron velocity, the flux equation reduces to a density equation:

$$n_e^*(x_{i+1}) = n_e^*(x_i) e^{(-\sigma^* n_{H2}(x_i)(x_{i+1}-x_i))} \tag{3}$$

where n_e^* is the subset of the electrons capable of causing emission, and σ^* is the effective attenuation cross section, σ_{total}/N^*. σ_{total} is the sum of the ionization, dissociation, and dissociative ionization cross-sections. N^* is the number of collisions required to bring the

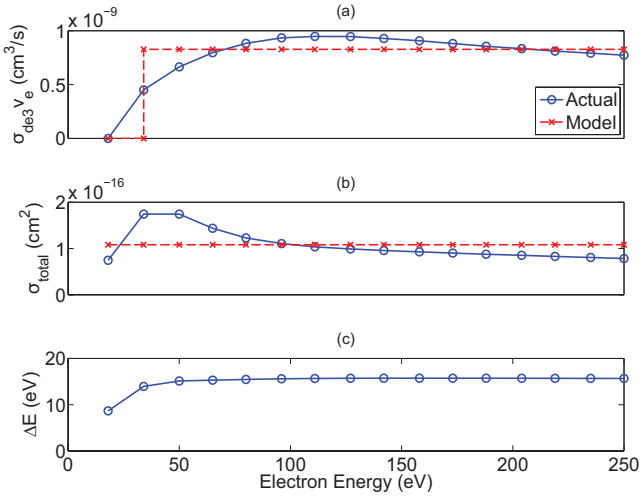

FIG. 2. (Color Online) a) $H^*(n = 3)$ production via dissociative excitation varies weakly and is approximated by a step function. b) The ionization cross-section is approximated by its mean value. c) The cross-section weighted energy loss for an electron.

electron energy below the emission threshold of 34eV. Above the threshold, σ_{total} is approximated as the mean value, $1.08x10^{-16}$cm^2 (see Figure 2b). The cross-section below the threshold is irrelevant, because low-energy electrons, including ionization product electrons, do not produce H_α emission. Figure 2c contains the cross-section weighted electron energy loss in a collision, ΔE, implying that for a 250eV beam, $N^* = 15$.

The description of the n_e^* population is simple: the electrons contribute equally to the H_α emission until they have undergone N^* collisions with molecules. This model allows an upper bound of the absolute molecular hydrogen density to be determined from an emission profile, even when the e-beam has been substantially depleted. At a point x_i with the densities $n_{H2}(x_i)$ and $n_e^*(x_i)$, $n_e^*(x_{i+1})$ is given by equation (3). Given equation (2), the molecular density at x_{i+1} is:

$$n_{H2}(x_{i+1}) = \frac{I(x_{i+1})}{I(x_i)} \frac{n_e^*(x_i)}{n_e^*(x_{i+1})} n_{H2}(x_i) \tag{4}$$

Choosing a starting point x_0, generally at the jet boundary, and taking an initial guess for $n_{H2}(x_0)$, Eqs. (3) and (4) are iterated from x_0 to an x_{final} that is the same distance from the jet center as x_0. For an axi-symmetric density profile, $n_{H2}(x_{final}) = n_{H2}(x_0)$. The value of $n_{H2}(x_0)$ is adjusted until this condition is satisfied, yielding the absolute density profile of

the jet. Because the drop in the emission only gives information on electrons that are pushed below the emission threshold, it underestimates the number of collisions and overestimates the gas density. However, in the real beam, this is mitigated by the fact that low energy electrons preferentially collide with molecules (see Figure 2b). A bound on the error in the hydrogen density is:

$$\eta = 1 - \frac{N^* \frac{I(x_0)-I(x_{final})}{I(x_0)}}{(x_{final} - x_0)\sigma_{total} < n_{H2} >} \tag{5}$$

The numerator is the number of collisions calculated by the method above, and the denominator estimates the total number of collisions using the calculated mean density, $< n_{H2} >$, across the region from x_0 to x_{final}. The actual number of collisions, and by extension the calculated density, will fall between these two estimates. The size of the band between them is sensitive to the degree of e-beam depletion, but typically within 25% for depletion less than 50%.

III. RESULTS AND DISCUSSION

Figure 3 is an example of a raw camera image from a 100psia backing pressure gas pulse. There is significant depletion of the e-beam, resulting in a left-right asymmetry in the emission profile. With the exception of some apparent broadening in regions of high intensity, the emission distribution in the z-direction is well described by a Gaussian with a full-width at half-maximum of 1.1cm. The broadening is an artifact of the optics and camera, not a real expansion of the e-beam. This is confirmed by measuring the same jet parameters with a reduced camera exposure time, which recovers the original emission width.

Figure 4a contains three emission profiles, from the final 1ms of a 4ms gas pulse of 50, 100, and 150psia backing pressures. A 3x3 pixel smoothing filter is applied to the raw camera data, and the emission is summed from $z = -1.5$ to $z = 1.5$cm, producing a linear distribution along the e-beam axis, i.e., $I(x, z) \rightarrow I(x)$. The 3cm window encompasses the entire e-beam width, and accommodates any artificial broadening. Using the method outlined above, the linear profiles are converted into the H_2 density profiles in Figure 4b. The starting point x_0 is chosen to be the emission peak at -2.1, -2.2, and -2.4cm, respectively, with $x_{final} = -x_0$. There is a clear "barrel shock" structure in the recovered profiles, as is expected for a supersonic jet expanded into vacuum.[13] As the backing pressure increases

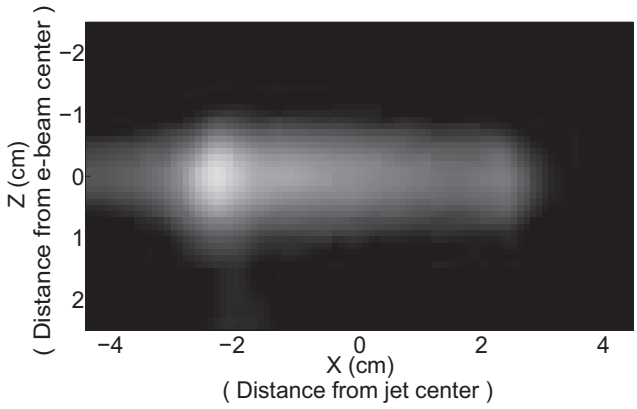

FIG. 3. Raw camera data of H_α emission from 100psia backing pressure gas pulse. The e-beam is 8.7cm below the nozzle outlet.

from 50-150psia, the barrel shock radius increases from 2.1 to 2.4cm, and the jet's central density increases from 1.3×10^{16} to $4.0 \times 10^{16}\text{cm}^{-3}$.

Even though the axi-symmetry condition is explicitly enforced for only one pair of points, the recovered profiles are highly left-right symmetric. The 50 and 100psia profiles are symmetric to within 2%. The 150psia profile is only symmetric to within 20%, reflecting a larger deviation from the simplified model for cases of severe beam depletion. Using equation (5), the 50, 100, and 150psia profiles have η of 18%, 25%, and 45%, which yield the error bands in Figure 4b. The highest density jet has largest error, due to the larger number of uncounted collisions.

To validate this method, an absolute calibration of the emission was performed. The chamber was pre-filled to a known pressure of 5mtorr of H_2, as measured with an MKS 222 Baratron, implying a number density of $1.6 \times 10^{14}\text{cm}^{-3}$ for room-temperature gas. The emission, smoothed and summed in the same manner as the data in Figure 4a, yields a conversion of $1.8 \times 10^{-13} \frac{counts \cdot cm^3 \cdot ms}{particles}$. $I(x_0)$ for the three profiles corresponds to peak densities of 1.2×10^{16}, 2.0×10^{16}, and $3.2 \times 10^{16}\text{cm}^{-3}$ for the 50, 100, and 150psia curves, respectively. The calibration densities are marked as discrete points in Figure 4b. $I(x_0)$ is used for the comparison because the beam depletion at x_0 is minimal. These calibration densities fall within the bands in Figure 4b, and so the attenuation model appears sound. While a more detailed physics model would reduce the width of the bands, the simplicity

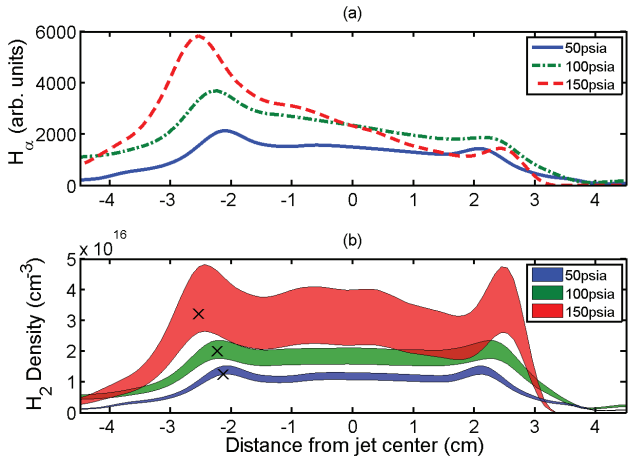

FIG. 4. (Color online) a) Original H_α emission profiles 8.7cm from the nozzle outlet. There is strong beam depletion at higher pressure. b) Recovered symmetric molecular density profiles. Absolute calibration values marked with "x".

of this model allows a straightforward calculation of the density. Future work will include simulations with a more detailed description of the electron population, to more precisely calculate the e-beam depletion rate and reduce the uncertainty in the absolute densities.

IV. ACKNOWLEDGEMENTS

Work supported by the U.S. Department of Energy under contract number DE-AC02-09CH11466.

REFERENCES

[1]L. Baylor, T.C. Jernigan, R.J. Colchin, G.L. Jackson, L.W. Owen, T.W. Petrie. J. Nucl. Mater. **313** 530 (2003)

[2]M. A. Mahdavi, R. Maingi, R. J. Groebner, A. W. Leonard, T. H. Osborne, and G. Porter. Phys. Plasmas, **10**, No. 10, (2003).

[3]R. Majeski, *et. al.* Nucl. Fusion **49** 055014 (2009)

[4]R.A. Smith,T. Ditmire, J.W.G. Tisch. Rev. Sci. Instrum., **69** 3798 (1998).

[5]A. Kramer, A. Kritzer, H. Reich, Th. Stohlker. Nucl. Instr. Meth. Phys. Res., **174** 205 (2001).

[6]L. Yao, *et. al.* Nuclear Fusion, **47** 1399 (2007).

[7]L.A. Gochberg. Prog. Aerosp. Sci. **33** (78), 431 (1997).

[8]S. Ya. Khmel', R. G. Sharafutdinov. Tech. Phys. **42** (3) (1997).

[9]W. Henkes, F. Mikosch. Int. J. Mass Spectrom. Ion Phys. **13**. 151 (1974).

[10]F. Dorchies, *et. al.* Phys. Rev. A **68** 023201 (2003).

[11]R.K. Janev, W.D. Langer, K. Evans, D.E. Post. *Elementary Processes in Hydrogen-Helium Plasmas*, Springer, (1987)

[12]F.F. Chen. *Introduction to Plasma Physics and Controlled Fusion*. Plenum Press, (1984)

[13]S. H. Be, K. Yano, H. Enjoji, K. Okamoto. Jpn. J. Appl. Phys. **14**, 1049 (1975).

The Princeton Plasma Physics Laboratory is operated
by Princeton University under contract
with the U.S. Department of Energy.

Information Services
Princeton Plasma Physics Laboratory
P.O. Box 451
Princeton, NJ 08543

Phone: 609-243-2750
Fax: 609-243-2751
e-mail: pppl_info@pppl.gov
Internet Address: http://www.pppl.gov